SYNTHETIC ASBESTOS INVESTIGATIONS, II: X-RAY AND OTHER DATA ON SYNTHETIC FLUOR-RICHTERITE, -EDENITE, AND -BORON EDENITE*

J. A. Kohn† and J. E. Comeforo,‡ *Electrotechnical Laboratory,*
U. S. Bureau of Mines, Norris, Tennessee.

Abstract

As a portion of a general research program on the synthesis of asbestiform minerals, x-ray and other data have been obtained on the following chemically analyzed synthetic fluor-amphiboles: richterite, $Na(CaNa)Mg_5(Si_4O_{11})_2F_2$, edenite, $NaCa_2Mg_5(Si_{3.5}Al_{0.5}O_{11})_2F_2$, boron edenite, $NaCa_2Mg_5(Si_{3.5}B_{0.5}O_{11})_2F_2$. Comparisons are made with the values previously reported for fluor-tremolite, $Ca_2Mg_5(Si_4O_{11})_2F_2$.

A detailed indexing of x-ray powder diffraction patterns has been made in the range up to 76° 2θ, and accurate unit cell dimensions have been determined. The observed cell-dimension variations are discussed with reference to ionic location and polarization. The synthesis and analysis of additional specified compositions are needed to elucidate the factors controlling fibrosity and flexibility in layered and allied silicate structures.

Introduction

During an extensive study of the synthesis of fluor-amphiboles from melts, over 100 different batch compositions were investigated; the effect of fluoride concentration and various isomorphic substitutions in the batch on the development of asbestiform amphibole were evaluated (1). Concurrently, some of the fundamental constants of various "end-members" of the monoclinic fluor-amphiboles were determined.

In the present study, the optical and x-ray constants of synthetic fluor-richterite, $Na(CaNa)Mg_5(Si_4O_{11})_2F_2$, fluor-edenite, $NaCa_2Mg_5(Si_{3.5}Al_{0.5}O_{11})_2F_2$, and a boron-containing fluor-edenite, $NaCa_2Mg_5(Si_{3.5}B_{0.5}O_{11})_2F_2$, have been evaluated and are compared with the values previously measured for synthetic fluor-tremolite, $Ca_2Mg_5(Si_4O_{11})_2F_2$ (2).

Experimental Procedure

The method of synthesis and the techniques employed were the same as previously reported (2); that is, a batch corresponding to the composition of the desired fluor-amphibole was melted and cooled, during which time the amphibole devitrified. Graphite crucibles with screw-on covers were used to minimize the extent of volatilization and to prevent the introduction of impurities that might enter the amphibole structure or otherwise cause a deviation from the desired composition.

The percentage of each raw material used in compounding the synthetic fluor-amphiboles is given in Table 1. To eliminate the presence of carbonates, hydroxides, or other compounds that decompose with liberation of gases, certain components were initially reacted to form stable, anhydrous, nonvolatile materials, such as $Na_2MgSi_3O_8$ (as glass), $CaSiO_3$, and MgB_2O_4. Others, such as the clay and silicic acid, were dehydrated before use. In every instance, the particle size of the ingredients was minus-100 mesh. After dry mixing in a glass jar with rubber balls, the batches were packed in the crucibles to hand tightness.

TABLE 1. FLUOR-AMPHIBOLE BATCH COMPOSITIONS (WEIGHT—PER CENT)

Raw Material	Richterite	Edenite	Boron edenite
$Na_2MgSi_3O_8$*	34.4	16.9	17.2
$CaSiO_3$*	14.1	27.7	28.2
MgF_2 (tech. grade)	7.6	7.5	7.6
MgO†	14.7	16.9	14.8
MgB_2O_4*	—	—	6.7
Dehydrated Georgia clay ($Al_2Si_2O_7$)	—	13.2	—
Dehydrated silicic acid† (SiO_2)	29.2	17.9	25.6
	100.0	100.1	100.1

* Prepared from reagent-grade chemicals.

† Reagent-grade chemicals.

The batches were fired to 1350° C., maintained at this temperature for 5 hours, and then cooled at 36° C. per hour to 1100° C., at which temperature the furnace was turned off. The resulting crystalline reaction products, consisting primarily of brittle, acicular crystals of fluor-amphibole (at least 80%), were ground to minus-200 mesh. Beneficiation was carried out by heavy-liquid separation using tetrabromoethane and methylene iodide (adjusted to 2.97 and 3.10 gm./cc., respectively) until fractions containing at least 95% fluor-amphibole (microscopically determined) were obtained. Each of these samples was divided into four aliquot portions: The first was examined petrographically, and the optical constants determined; the second was chemically analyzed; the third was used for the x-ray study; and the last portion was filed.

RESULTS

(1) *Chemical Composition*

The beneficiated samples of the synthetic fluor-amphiboles were examined petrographically, and in no case was the estimate of the total

TABLE 2. CHEMICAL ANALYSES OF SYNTHETIC FLUOR-AMPHIBOLES*

Constituent	Fluor-richterite		Fluor-edenite		Fluor-boron edenite	
	Theoretical	Actual	Theoretical	Actual	Theoretical	Actual
SiO_2	58.45	58.88	50.17	51.09	51.16	52.21
Al_2O_3	.00	—	6.08	6.47	.00	—
B_2O_3	.00	—	.00	—	4.24	3.91
Fe_2O_3	.00	0.17	.00	.21	.00	.24
MgO	24.51	24.24	24.05	23.06	24.52	24.09
CaO	6.82	7.00	13.38	12.30	13.64	12.69
Na_2O	7.54	7.20	3.70	4.26	3.77	3.99
F^-	4.62	4.74	4.53	4.89	4.62	4.85
$O = F$	−1.94	−2.00	−1.91	−2.06	−1.95	−2.04
	100.00	100.23	100.00	100.22	100.00	99.94

* Analysts: H. R. Shell, R. L. Craig; samples No. 3848, 3867, and 3850, respectively. Analytical data based on samples dried at 110° C.

impurities greater than 4%. The fluor-richterite sample contained less than 1% impurity, mostly CaF_2. In the case of fluor-edenite, the major contaminant was 1–2% pyroxene, probably diopside. The remaining impurity concentration was less than $\frac{1}{2}$%. The extraneous phases in fluor-boron edenite totaled less than 4%, of which approximately 3% was forsterite.

The chemical analyses of the beneficiated samples are given in Table

TABLE 3. COMPARISONS OF THEORETICAL AND EMPIRICAL IONIC RATIOS OF SYNTHETIC FLUOR-AMPHIBOLES

	(WO_{12})	(XO_8)	(YO_6)	(ZO_4)	
			Richterite		
Theoretical	Na	(CaNa)	Mg_5	Si_8	$O_{22}F_2$
Calculated*	$Na_{0.93}$	$(Ca_{1.03}Na_{0.97})$	$Mg_{4.93}$	$Si_{8.04}$	$O_{22}F_{2.04}$
			Edenite		
Theoretical	Na	Ca_2	Mg_5	(Si_7Al)	$O_{22}F_2$
Calculated*	$Na_{0.99}$	$(Ca_{1.84}Na_{0.16})$	$(Mg_{4.79}Al_{0.18})$	$(Si_{7.12}Al_{0.88})$	$O_{22}F_{2.15}$
			Boron edenite		
Theoretical	Na	Ca_2	Mg_5	(Si_7B)	$O_{22}F_2$
Calculated*	$Na_{0.93}$	$(Ca_{1.87}Na_{0.13})$	$Mg_{4.92}$	$(Si_{7.16}B_{0.92})$	$O_{22}F_{2.10}$

* Calculated from chemical analysis on basis of 22 oxygen atoms. No attempt was made to correct for the small amounts of impurities present.

2. A comparison between the theoretical and empirical formulas of the three fluor-amphiboles appears in Table 3.

(2) *Optical Properties*

Comparisons of the optical constants reported on various naturally occurring richterites and edenites with those measured on the synthetic fluor-amphiboles are rendered difficult because the natural minerals invariably contain significant amounts of cations other than those required for theoretical compositions (3, 4). For this reason, the observed differences cannot be attributed entirely to complete replacement of hydroxyl by fluoride.

The refractive indices of the synthetic fluor-amphiboles were measured at room temperature with a petrographic microscope, using the oil-immersion technique. The results obtained are compared in Table 4 with those previously measured for synthetic fluor-tremolite.

TABLE 4. SYNTHETIC FLUOR-AMPHIBOLE OPTICAL CONSTANTS*

	Tremolite	Richterite†	Edenite‡	Boron-edenite
X	1.581	1.603	1.605	1.588
Y	1.593	1.614	1.617	1.598
Z	1.602	1.622	1.624	1.605
$Z \wedge c$	21°	22°	18°	12°
2V	$86\frac{1}{2}°$	72°	69°	75°
Sign	(−)	(−)	(−)	(−)

* Determinations by M. V. Denny; maximum error for X, Y, and Z is ±0.002; 2V determined by means of a 5-axis universal stage, using sodium (*D*) light.

† A natural richterite ("soda-tremolite") described by Larsen (3) was not used for comparison of optical properties owing to the presence of 3.91% Fe_2O_3 and 2.44% FeO.

‡ A natural, biaxial positive edenite described by Palache (4) was not used for comparison of optical properties owing to the presence of 1.02% Fe_2O_3 and 3.38% FeO.

(3) *X-ray Data*

No x-ray data are available in the literature on relatively pure synthetic or natural amphiboles of the types herein concerned. In the present study, accurate unit cell dimensions have been obtained, and complete diffraction data are given in the range up to 76° 2θ. The three synthetic fluor-amphiboles studied are monoclinic, with a bimolecular unit cell.

All x-ray diffraction data were recorded using a chart operation in conjunction with a Philips high-angle goniometer (diffractometer). The synthetic fluor-amphibole samples were packed in the usual rectangular aluminum holders. The instrumental setting used was as follows: scale factor, 16 (unless rescanning a very strong maximum); multiplier, 1.0

(giving a counting rate of 800 counts per second, full scale); time constant, 4 seconds; Geiger overvoltage, 300 volts; divergence slit, 1°; scanning speed, $\frac{1}{4}$° per minute; chart scale, $\frac{1}{2}$ inch per degree.

Both before and after each chart operation involving a fluor-amphibole pattern, appropriate silicon maxima were recorded using the silicon standard compact furnished with the instrument. Corrections ranged from 0.005° to 0.055° and were read from a curve plotting instrumental correction against 2θ.

A low-power microscope fitted with a movable-hair ocular, used in conjunction with a photographically processed slide of 200 lines per inch, permitted very accurate 2θ readings of the diffraction maxima. For those peaks directly concerned with the calculation of the unit-cell dimensions, 2θ readings to the third decimal place were obtained. For all other maxima, measurements were taken to 0.005°. Following the procedure established by Donnay and Donnay (5), the peaks were bisected at approximately two-thirds of the peak height to obtain the readings.

In the case of fluor-tremolite, the positions of the maxima directly involved in the calculation of the cell dimensions were determined by a counting operation in conjunction with the Philips unit. For the present study, a chart operation was found to be of approximately the same accuracy (see Table 8) and substantially less time-consuming. After the complete pattern of the fluor-amphibole under investigation was obtained by scanning down-scale from 76° 2θ, four sharp, unambiguously-indexed maxima in the higher 2θ range were selected. Each chosen peak was then scanned four additional times. 2θ values averaged from the 5 separate measurements were used for a solution of the quadratic form (6). The unit-cell dimensions thus derived were refined until close agreement was obtained between the calculated and observed 2θ values of various selected maxima. The final cell dimensions are given in Table 9 and compared with those previously obtained for synthetic fluor-tremolite.

Following the last cell-dimension refinement, the positions of all reflections permissible by the space group symmetry ($C\ 2/m$) were calculated in the range up to 76° 2θ (approximately 250 potential maxima in each case). The diffraction data for all resolved maxima (and a few significant doublets) in this range are tabulated in Tables 5, 6, and 7 for synthetic fluor-richterite, -edenite, and -boron edenite, respectively. Results bearing on the accuracy of the diffraction data, and ultimately upon the unit-cell dimensions adopted, are collected in Table 8, and compared with the values for synthetic fluor-tremolite. In the present study, no diffraction maximum showed a deviation in 2θ of more than 0.02° from the calculated value, and the average deviation was in the order of 10^{-4} degrees.

hkl	2θ obs.	2θ calc.*	Δ2θ	Meas. Int.	d calc.
020	9.865°	9.855°	−0.01°	3	8.979 Å
110	10.51	10.515	+ .005	>100	8.409
130	17.49	17.50	+ .01	2	5.067
11$\bar{1}$	18.25	18.255	+ .005	3	4.860
200	18.635	18.645	+ .01	11	4.759
040	19.76	19.775	+ .015	10	4.489
220	21.115	21.13	+ .015	4	4.205
111	22.275	22.265	− .01	2	3.993
13$\bar{1}$	23.03	23.045	+ .015	4	3.859
131	26.34	26.345	+ .005	10	3.380
150	26.505	26.505	0	3	3.360
240	27.285	27.285	0	60	3.265
310	28.54	28.55	+ .01	≫100	3.124
221	30.325	30.33	+ .005	11	2.944
15$\bar{1}$	30.505	30.52	+ .015	3	2.926
330	31.91	31.91	0	76	2.803
33$\bar{1}$	32.91	32.89	− .02	9	2.721
151	33.15	33.15	0	20	2.700
061	34.73	34.715	− .015	7	2.582
20$\bar{2}$	35.555	35.535	− .02	6	2.524
350	37.805	37.805	0	11	2.378
35$\bar{1}$	38.68	38.665	− .015	7	2.327
42$\bar{1}$	38.885	38.875	− .01	5	2.315
17$\bar{1}$	39.385	39.365	− .02	7	2.287
171	41.515	41.50	− .015	3	2.174
132	41.63	41.64	+ .01	3	2.167
261	41.81	41.81	0	8	2.159
202	44.20	44.195	− .005	3	2.048
351	44.905	44.91	+ .005	5	2.017
370	45.435	45.43	− .005	5	1.9947
190	46.465	46.46	− .005	3	1.9528
510	48.03	48.025	− .005	29	1.8928
19$\bar{1}$	49.06	49.05	− .01	3	1.8556
530	50.275	50.255	− .02	8	1.8139
0·10·0	50.815	50.80	− .015	2	1.7957
51$\bar{2}$	52.575	52.585	+ .01	2	1.7389
461	55.67	55.67	0	16	1.6496
480	56.295	56.295	0	6	1.6327
1·11·0	57.20	57.205	+ .005	10	1.6090
600	58.10	58.105	+ .005	9	1.5862
55$\bar{2}$	58.695	58.715	+ .02	3	1.5711
620	59.105	59.09	− .015	2	1.5620
551	61.68	61.675	− .005	6	1.5026
0·12·0	61.96	61.955	− .005	7	1.4964
442	63.10	63.10	0	1	1.4721
3·11·0	64.08	64.095	+ .015	5	1.4516
66$\bar{1}$	64.975	64.98	+ .005	11	1.4340
512	68.545	68.555	+ .01	6	1.3676
60$\bar{3}$⎫ 532⎭	70.355	70.355⎫ 70.355⎭	—	1	1.3370⎧ 1.3369⎩
263	70.575	70.575	0	1	1.3333
75$\bar{1}$	72.23	72.23	0	3	1.3068
2·12·$\bar{2}$	73.495	73.505	+ .01	4	1.2872

* Using λ CuKα₁ (1.54050 A) above 25° 2θ and λ CuKα (1.5418 A) below 25° 2θ.

J. A. KOHN AND J. E. COMEFORO

TABLE 6. X-RAY DIFFRACTION DATA (POWDER) FOR SYNTHETIC FLUOR-EDENITE
(*Space Group C 2/m*)

hkl	2θ obs.	2θ calc.*	$\Delta 2\theta$	Meas. Int.	d calc.
020	9.825°	9.825°	0°	4	9.002 Å
110	10.515	10.515	0	81	8.413
11$\bar{1}$	18.15	18.17	+ .02	2	4.882
200	18.64	18.645	+ .005	3	4.759
040	19.71	19.725	+ .015	6	4.501
220	21.095	21.115	+ .02	6	4.208
131⎱	26.37	⎧26.37 ⎱	—	10	⎧3.377
041⎰		⎩26.375⎰			⎩3.376
240	27.24	27.245	+ .005	42	3.270
310	28.54	28.54	0	99	3.125
221⎱	30.395	⎧30.405⎱	—	19	⎧2.937
15$\bar{1}$⎰		⎩30.415⎰			⎩2.936
330	31.87	31.875	+ .005	37	2.805
33$\bar{1}$	32.74	32.735	− .005	7	2.733
151	33.135	33.14	+ .015	15	2.701
061	34.645	34.645	0	7	2.587
20$\bar{2}$	35.37	35.36	− .01	11	2.536
170	36.145	36.145	0	1	2.483
40$\bar{1}$	37.35	37.35	0	2	2.406
350	37.76	37.755	− .005	8	2.381
35$\bar{1}$	38.51	38.50	− .01	7	2.336
42$\bar{1}$	38.70	38.71	+ .01	7	2.324
17$\bar{1}$	39.24	39.24	0	5	2.294
261	41.815	41.815	0	9	2.158
351	44.95	44.96	+ .01	8	2.014
370	45.36	45.35	− .01	3	1.9980
190	46.325	46.34	+ .015	2	1.9577
510	48.02	48.015	− .005	12	1.8932
46$\bar{1}$	48.47	48.46	− .01	1	1.8769
530	50.25	50.235	− .015	6	1.8146
$0 \cdot 10 \cdot 0$	50.665	50.66	− .005	1	1.8004
550	54.485	54.475	− .01	2	1.6830
461	55.735	55.72	− .015	12	1.6481
480	56.205	56.21	+ .005	4	1.6351
$1 \cdot 11 \cdot 0$	57.03	57.045	+ .015	3	1.6130
600	58.095	58.09	− .005	4	1.5865
402	59.46	59.445	− .015	2	1.5535
551 ⎱	61.79	⎧61.77⎱	—	12	⎧1.5006
$0 \cdot 12 \cdot 0$⎰		⎩61.78⎰			⎩1.5003
$2 \cdot 10 \cdot \bar{2}$	63.305	63.29	− .015	1	1.4681
$3 \cdot 11 \cdot 0$	63.95	63.945	− .005	2	1.4546
66$\bar{1}$	64.76	64.77	+ .01	11	1.4381
51$\bar{2}$	68.80	68.785	− .015	5	1.3636
710	69.24	69.23	− .01	2	1.3560
75$\bar{1}$	72.01	72.015	+ .005	3	1.3102
$2 \cdot 12 \cdot \bar{2}$	73.235	73.24	+ .005	2	1.2913

* Using λ CuKα_1 (1.54050 Å) above 25° 2θ and λ CuK$_\alpha$ (1.5418 Å) below 25° 2θ.

TABLE 7. X-Ray Diffraction Data (Powder) for Synthetic Fluor-Boron Edenite
(*Space Group* C 2/m)

hkl	2θ obs.	2θ calc.*	Δ2θ	Meas. Int.	d calc.
020	9.845°	9.85°	+0.005°	4	8.979 Å
110	10.54	10.54	0	95	8.395
130	17.50	17.515	+ .015	3	5.064
11$\bar{1}$	18.255	18.255	0	2	4.860
200	18.675	18.685	+ .01	8	4.748
040	19.755	19.775	+ .02	6	4.489
220	21.155	21.165	+ .01	5	4.198
111	22.325	22.305	− .02	2	3.986
13$\bar{1}$	23.04	23.045	+ .005	3	3.859
131	26.39	26.38	− .01	7	3.376
240	27.31	27.315	+ .005	35	3.262
310	28.61	28.61	0	≫100	3.118
221	30.405	30.395	− .01	16	2.939
330	31.955	31.955	0	29	2.798
33$\bar{1}$	32.925	32.91	− .015	9	2.719
151	33.18	33.175	− .005	20	2.698
350	37.85	{37.85	—	6	{2.375
400		37.86}			2.374}
35$\bar{1}$	38.675	38.68	+ .005	8	2.326
42$\bar{1}$	38.915	38.92	+ .005	6	2.312
17$\bar{1}$	39.375	39.365	− .01	4	2.287
261	41.86	41.855	− .005	7	2.156
351	45.00	44.985	− .015	5	2.013
370	45.47	{45.47	—	5	{1.9931
222		45.47}			1.9929}
190	46.48	46.465	− .015	2	1.9526
510	48.13	48.13	0	19	1.8888
19$\bar{1}$	49.04	49.05	+ .01	2	1.8556
530	50.37	50.36	− .01	9	1.8104
0·10·0	50.805	50.80	− .005	2	1.7957
461	55.76	55.77	+ .01	8	1.6469
60$\bar{1}$	56.36	{56.355	—	5	{1.6312
480		56.36}			1.6311}
1·11·0	57.185	57.205	+ .02	3	1.6089
600	58.235	58.24	+ .005	7	1.5828
620	59.235	59.225	− .01	2	1.5588
402	59.39	59.39	0	2	1.5549
0·12·0	61.96	61.955	− .005	5	1.4964
3·11·0	64.115	64.13	+ .015	2	1.4509
66$\bar{1}$	65.065	65.065	0	13	1.3423
512	68.765	{68.735	—	3	{1.3645
73$\bar{1}$		68.77}			1.3639}
710	69.41	69.41	0	3	1.3528
730	71.205	71.205	0	2	1.3231
75$\bar{1}$	72.355	72.345	− .01	3	1.3050
2·12·$\bar{2}$	73.50	73.51	+ .01	2	1.2872

* Using λ CuKα_1 (1.54050 Å) above 25° 2θ and λ CuKα (1.5418 Å) below 25° 2θ.

TABLE 8. ACCURACY OF SYNTHETIC FLUOR-AMPHIBOLE DIFFRACTION DATA

	Maximum Deviation (degrees)	Average Deviation (degrees)	Contributing Peaks (number)
Tremolite	0.03	$+2.5 \times 10^{-4}$	41
Richterite	.02	-4.0×10^{-4}	51
Edenite	.02	-2.5×10^{-4}	40
Boron edenite	.02	$+1.3 \times 10^{-4}$	38
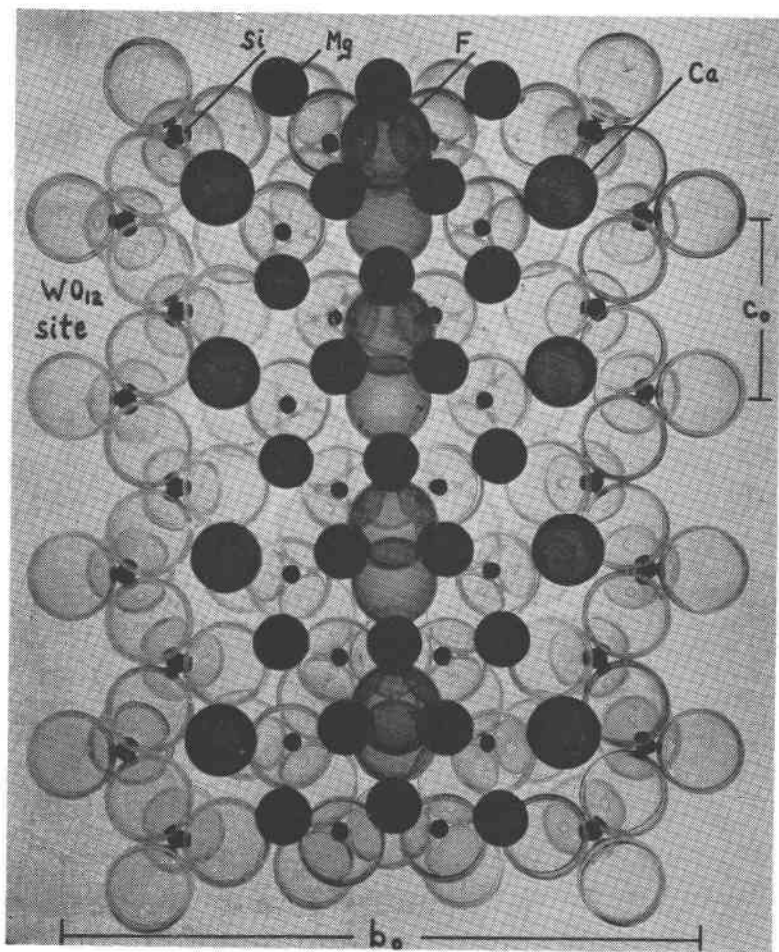
FIG. 1. Plastic-ball model (8) of a portion of the fluor-tremolite structure, with $[d_{100}]$ perpendicular to the plane of the figure.

Discussion

A model of a portion of the fluor-tremolite structure, as derived by Warren (7), is depicted in Fig. 1 to supplement the following discussion.

In richterite, $Na(CaNa)Mg_5(Si_4O_{11})_2F_2$, the substitution of 2 Na^+ for 1 Ca^{++} presents two geometrical possibilities for the sites occupied by these cations. Specifically, 1 Na^+ can fill the 12-fold vacant sites known to exist in tremolite (environment similar to the 12-fold positions in mica), while the remaining Na^+ proxies for Ca^{++} in 8-fold coordination. On the other hand, both Na^+ ions may replace Ca^{++} in the (XO_8) positions, with Ca^{++} occupying the (WO_{12}) vacant sites. In tremolite, where the Ca^{++} ions are more or less free to choose between 12- and 8-fold coordination, the latter is preferred, although in calcium phlogopite, $Ca_2Mg_6(Si_3AlO_{10})_2F_4$, where no such option exists, Ca^{++} does occupy the position of 12-fold coordination. Thus it would seem that in the particular structural environment presented by the tremolite arrangement, Ca^{++} is more stable in the (XO_8) position. Since the structural environment of richterite does not differ radically from that of tremolite, it seems logical to assume that, where possible, Ca^{++} will again seek positions of 8-fold coordination. Thus it is indicated that Na^+ occupies the (WO_{12}) vacant sites, and the (XO_8) positions are shared by both Na^+ and Ca^{++}. This double coordination of Na^+ is not unusual, as shown by eckermannite, $NaNa_2Mg_4Al(Si_4O_{11})_2(OH,F)_2$, where the (WO_{12}) and (XO_8) positions are filled by this cation.

TABLE 9. MONOCLINIC CELL DIMENSIONS OF SYNTHETIC FLUOR-AMPHIBOLES*

	Tremolite	Richterite	Edenite	Boron edenite
a_0	9.781 Å	9.823	9.847	9.807
b_0	18.007	17.957	18.004	17.957
c_0	5.267	5.268	5.282	5.266
β	75°29′	75°40′	75°10′	75°33′
Calculated Density	3.021 g/cm³	3.035	3.077	3.042

* Maximum errors are as follows: a_0, ±0.005; b_0, ±0.004; c_0, ±0.006; β, ±5′; calculated density (D_x), ±0.006.

The change in unit-cell dimensions between tremolite and richterite, as shown in Table 9, can be explained by either of the above assumptions. Both would result in an increased a dimension because of filling of the vacant sites, since $[d_{100}]$ parallels the principal axis of the (WO_{12}) coordination polyhedron. With the limited data available, the contraction along b can be ascribed to substitution of a slightly smaller ion (Na^+ for

Ca^{++}) in positions between the double chains. Regardless of the actual location of the Na^+ and Ca^{++} ions, no noticeable change in the c direction would result, as the latter parallels the elogation of the Si_4O_{11} chains and is essenitally uninfluenced by the occupants of the (WO_{12}) and (XO_8) positions. Knowledge of the cell dimensions of fluor-eckermannite and various richterites, especially those in which Mn^{++}, Ba^{++}, or Sr^{++} replace Ca^{++}, might resolve this question without recourse to a detailed structural analysis.

Edenite, $NaCa_2Mg_5(Si_{3.5}Al_{0.5}O_{11})_2F_2$, is derived from tremolite by substituting one Al^{+3} for Si^{+4} in tetrahedral coordination and restoring electrical neutrality by filling the (WO_{12}) sites with Na^+. In boron edenite, $NaCa_2Mg_5(Si_{3.5}B_{0.5}O_{11})_2F_2$, B^{+3} replaces Al^{+3} in the (ZO_4) positions. As with richterite, filling of the 12-fold sites in both edenites increases the a dimension relative to that observed in tremolite (cf. Table 9). This direction is also influenced by the substitution in 4-fold coordination. Thus the a dimension of aluminum edenite is larger than that of boron edenite, owing to the larger $(AlO_4)^{-5}$ grouping. It was expected that this difference in tetrahedron size between $(AlO_4)^{-5}$ and $(BO_4)^{-5}$ would also be reflected in the b direction, with aluminum edenite exhibiting the larger b dimension. The observed data bear out this expectation. When compared with fluor-tremolite, however, the b dimension of aluminum edenite remains essentially the same. This may be due either to a cushioning effect along b (perpendicular to the direction of the double chains) or to a distortion of the $(AlO_4)^{-5}$ grouping, which would not be unexpected with a trivalent ion in 4-fold coordination.

The c dimension of aluminum edenite is increased relative to that of tremolite owing to the effect of the larger $(AlO_4)^{-5}$ grouping on the direction of the double chains. In boron edenite a contraction (relative to tremolite) was expected along c, because of the probable smaller size of the $(BO_4)^{-5}$ grouping in comparison to $(SiO_4)^{-4}$.* This contraction, however, did not materialize, which intimates a distortion on the $(BO_4)^{-5}$ tetrahedron. Such a distortion would be in keeping with the relative ease of polarization of this group. The indicated distortions of both the $(AlO_4)^{-5}$ and $(BO_4)^{-5}$ groups are such that the tetrahedra seem attenuated (relative to b) along the c direction.

In the discussion of the fluor-richterite composition, certain isomorphic substitutions were suggested as offering promise in correlating unit-cell dimensions with ionic location. Continuing in this vein, the effect of polarization of the tetrahedra could be clarified by the synthesis and

* Analogous to the relative sizes of the $(BO_4)^{-5}$ and $(SiO_4)^{-4}$ tetrahedra in danburite, $CaB_2Si_2O_8$(9).

analysis of amphiboles and micas in which various cations, such as Be^{++}, Ge^{+4}, and V^{+3}, substitute for Si^{+4}. In a number of instances such compositions have been prepared in this laboratory, but samples pure enough for investigation have not been obtained. Likewise, additional data are needed to understand fully the effect of the replacement of $(OH)^-$ by F^-, (10) which is basic to the study of fluor-silicates.

When such data become available, it may be possible to comprehend the relationships existing among the many layered and allied silicate minerals. This, in turn, by clarifying the directional distribution of bond strengths, especially those perpendicular to the layers or chains, would shed light on the ultimate problems of fibrosity and flexibility and their relation to crystal structure.

ACKNOWLEDGMENTS

REFERENCES

1. COMEFORO, J. E., EITEL, WILHELM, AND HATCH, R. A. (1954), Synthetic asbestos investigations, III: The effect of isomorphic substitutions and fluoride concentration on the synthesis of fluor-amphiboles: To be published as *U. S. Bur. Mines. Rept. Invest.*

2. COMEFORO, J. E. AND KOHN, J. A., (1954), Synthetic asbestos investigations, I: Study of synthetic fluor-tremolite: *Am. Mineral.*, **39**, 537–548.

3. LARSEN, E. S. (1942), Alkalic rocks of Iron Hill, Gunnison County, Colo.: *U. S. Geol. Surv. Prof. Paper* **197A**, 64 pp.

4. PALACHE, C. (1935), The minerals of Franklin and Sterling Hill, Sussex County, New Jersey: *U. S. Geol. Surv. Prof. Paper* **180**, 135 pp. (particularly p. 73).

5. DONNAY, GABRIELLE, AND DONNAY, J. D. H. (1952), The symmetry change in the high-temperature alkali-feldspar series: *Am. J. Sci., Bowen Vol.*, 115–132 (particularly p. 118).

6. (1944), Internationale Tabellen zur Bestimmung von Kristallstrukturen: Gebrüder Borntraeger, Berlin, vol. II, revised ed., 454.

7. WARREN, B. E. (1929), The structure of tremolite, $H_2Ca_2Mg_5(SiO_3)_8$: *Z. Krist.*, **72**, 44.

8. HATCH, R. A., COMEFORO, J. E., AND PACE, N. A. (1952), Transparent, plastic-ball, crystal structure models: *Am. Mineral.*, **37**, 58–67.

9. HERMANN, C., et al (1937), Strukturbericht, vol. II (1928–1932), 153–155.

10. KOHN, J. A., AND HATCH, R. A. (1955), Synthetic mica investigations, VI: X-ray and optical data on synthetic fluor-phlogopite: *Am. Mineral.*, **40**, 10–21.

Manuscript received May 20, 1954.